Citation: Molecular Therapy—Nucleic Acids (2016) 5, e334; doi:10.1038/mtna.2016.48
Official journal of the American Society of Gene & Cell Therapy
www.nature.com/mtna

LETTER TO THE EDITOR

GFP to BFP Conversion: A Versatile Assay for the Quantification of CRISPR/Cas9-mediated Genome Editing

Molecular Therapy—Nucleic Acids (2016) **5**, e334; doi:10.1038/mtna.2016.48; published online 12 July 2016

A RAPID ASSAY FOR GENOME EDITING EFFICIENCY

To the Editor: Genome editing via programmable endonucleases enables us to generate site-specific double-strand breaks at virtually any position in a target genome.[1–3] Exploiting cellular repair mechanisms, this can be used for targeted gene disruption via nonhomologous end joining (NHEJ) or for the precise manipulation of a target sequence through homology-directed repair (HDR) in the presence of a suitable DNA template. The latter carries great promise for the field of gene therapy as it can be utilized for the correction of disease-causing mutations. Earlier this year, De Ravin *et al.* reported HDR rates >50% in human hematopoietic stem and progenitor cells using zinc finger nucleases, demonstrating that therapeutic levels of gene correction can be achieved in clinically relevant cell types.[4] However, the efficiency of HDR remains considerably lower than that of NHEJ in many experimental settings and a background of mutagenic NHEJ is currently limiting the usefulness of genome editing for gene therapy approaches. This limitation signifies a need to identify conditions that bias genome editing toward HDR. Strategies have been developed to encourage HDR over NHEJ, including stimulation with small molecules and inhibition or disruption of DNA ligase 4 activity, but optimal conditions still need to be established.[5–7] Reliable quantification of HDR and NHEJ is essential to the identification of conditions that favor HDR over NHEJ. This was first achieved through the generation of single-cell clones,[2] which is impractical for the determination of overall NHEJ and HDR frequencies. The Traffic Light Reporter system provided the first fluorescence-based assay for the simultaneous quantification of HDR and NHEJ.[8] However, this system requires the generation of reporter cell lines and therefore can not be applied easily in primary cells or animal models. Sophisticated methods such as single molecule real time sequencing or sib-selection/droplet digital polymerase chain reaction allow for the quantification of HDR and NHEJ at endogenous loci without the necessity of generating individual clones.[9,10] However, downstream sample processing requirements limit the use of these techniques in a high-throughput format. As an alternative, we propose a simple strategy for the simultaneous quantification of HDR and NHEJ by targeting the ubiquitous enhanced green fluorescent protein (EGFP) fluorescent reporter (**Figure 1a**, **b**).

In 1994, Heim *et al.* discovered that a single base substitution (196T > C) in the chromophore of wild-type (wt) GFP could shift its fluorescence absorption and emission toward the blue spectrum, thus creating blue fluorescent protein (BFP).[11] Here, we demonstrate that EGFP can be converted into BFP in EGFP-expressing cell lines using the clustered regularly interspaced short palindromic repeats (CRISPR) and CRISPR-associated protein 9 (Cas9) system. HDR and NHEJ can subsequently be quantified as blue fluorescence and loss of fluorescence, respectively. K562 cells carrying an EGFP-modified human β-globin locus in the AAVS-1 site in chromosome 19,[12] and HEK293T cells that were stably transduced with an integration competent lentiviral EGFP expression construct (K562-50 and HEK293T-EGFP, **Figure 2a**) were used in this study. Two guide RNA (gRNA) vectors based on px330-IRES mCherry were designed to target Cas9 into close proximity to the target site (**Figure 1b**). A double-stranded BFP PCR reaction product amplified from the vector pLMP (primers 5′-CCTGAAGTTCATCTGC ACCACC-3′ and 5′-GACGTAGCCTTCGGGCATGG-3′) was compared with two single-stranded repair templates (ssODN) (**Figure 1c**). The gRNA/Cas9 plasmids (5 µg) and HDR templates (100 pmol) were coelectroporated into the target cells using a BioRad Gene Pulser II electroporator. GFP and BFP fluorescence were assessed 10 days later using flow cytometry. HDR and NHEJ were quantified as the percentage of BFP^+ cells and nonfluorescent cells, respectively. HDR/total editing ratios (R) were determined using the formula: R = (HDR)/(NHEJ + HDR) * 100.

Our data shows that a single 196T > C substitution using ssODN1 is sufficient to convert *GFP* to *BFP*. However, low fluorescence intensity and a low HDR frequency were observed in comparison with the other templates in K562-50 cells (**Figure 1d**,**e**). An additional 194C > G substitution in ssODN2, corresponding to a reversion of the EGFP amino acid sequence back to that of wild-type GFP, was sufficient to restore BFP fluorescence intensity to that observed with the PCR template (**Figure 1e**). The low HDR frequency observed with ssODN1 was theorized to result from recutting of the repaired sequence by Cas9, as the sequence resulting from HDR retains the complete target sequence for gRNA1 and contains only one mismatch in the gRNA2 target site. The 194C > G substitution introduces an additional mismatch in the gRNA2 target site and eliminates the gRNA1 protospacer adjacent motif sequence. To further reduce the target sequence similarity with gRNA1 after HDR, ssODN2 was designed with an

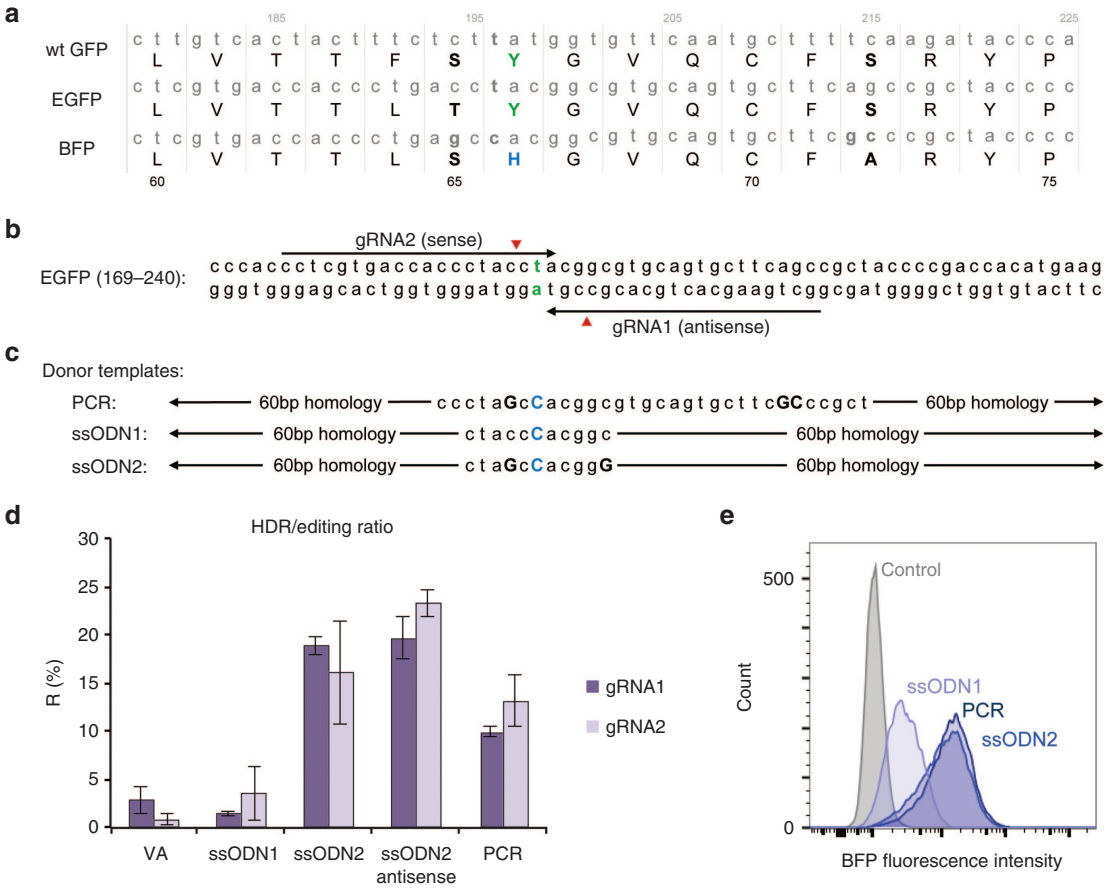

Figure 1 HDR template optimization. (**a**) Multiple sequence alignment between the wtGFP, EGFP, and BFP chromophore regions. A single Y66H amino acid substitution corresponds to a shift in the fluorescence excitation and emission spectra of the protein, converting GFP to BFP. (**b**) Gene targeting strategy. Two gRNAs, in sense and antisense orientation relative to the EGFP coding sequence, target Cas9 to the EGFP chromophore. Cleavage sites are marked by red indicators, targeted nucleotide is highlighted in green. (**c**) A dsDNA PCR product amplified from a BFP plasmid (153 base pair) and two ssODN (133 nucleotides) were used as templates for HDR. Capital letters indicate deviations from the EGFP target sequence. (**d**) Influence of the HDR template on relative HDR rates. K562-50 cells were coelectroporated with a plasmid encoding Cas9 and either gRNA1 or gRNA2 and different HDR templates. Ten days postelectroporation, HDR and NHEJ were measured as BFP fluorescence and loss of fluorescence, respectively. Graph represents HDR/total editing ratios and SDs of two independent experiments (VA = no HDR template). (**e**) Fluorescence intensities of HDR products using different HDR templates. The BFP PCR product and ssODN2 yield a HDR product of ~3× greater fluorescence than ssODN1. Histograms show fluorescence intensities of BFP+ cells sorted via fluorescence-activated cell sorting after GFP to BFP conversion with different HDR templates compared with nonfluorescent cells resulting from NHEJ without a HDR template (control).

additional silent mutation (201C > G). In accordance with our expectations, the highest HDR frequency was achieved with ssODN2 in both K562-50 and HEK293T-EGFP cells (5.8% and 23.3%, respectively, **Figure 2a**). No significant difference was observed between sense and antisense configuration of ssODN2 (**Figure 1d**). The assay was validated through sequencing of clones grown from the GFP$^+$, BFP$^+$, and nonfluorescent populations after editing with gRNA1 and ssODN2 in K562-50 cells (**Figure 2b**).

In summary, we demonstrate that GFP to BFP conversion is a reliable and simple method for the quantification of HDR and NHEJ. The high sensitivity of the GFP chromophore region to single amino acid deletions demonstrated by Arpino *et al.* supports our hypothesis that even +3 and −3 insertions/deletions can be detected as loss of fluorescence.[13] We have applied this to the optimization of a HDR template for GFP to BFP conversion and verified the strategy through sequencing. While we used EGFP$^+$ cells as targets, wt GFP may also be a target in place of EGFP. This strategy could be used in a high-throughput screen to identify conditions that enhance HDR frequency (**Figure 2c**). In order to address mechanistic differences that uniquely affect genome-editing rates dependent on the donor template used, the screen can easily be adapted to use a different template type (*e.g.*, dsDNA, adeno-associated virus). The abundance of EGFP-expressing cell lines and animal models permit the application of this strategy for optimization of HDR in a wide range of primary and transformed cells for the establishment of *in vivo* gene repair strategies.

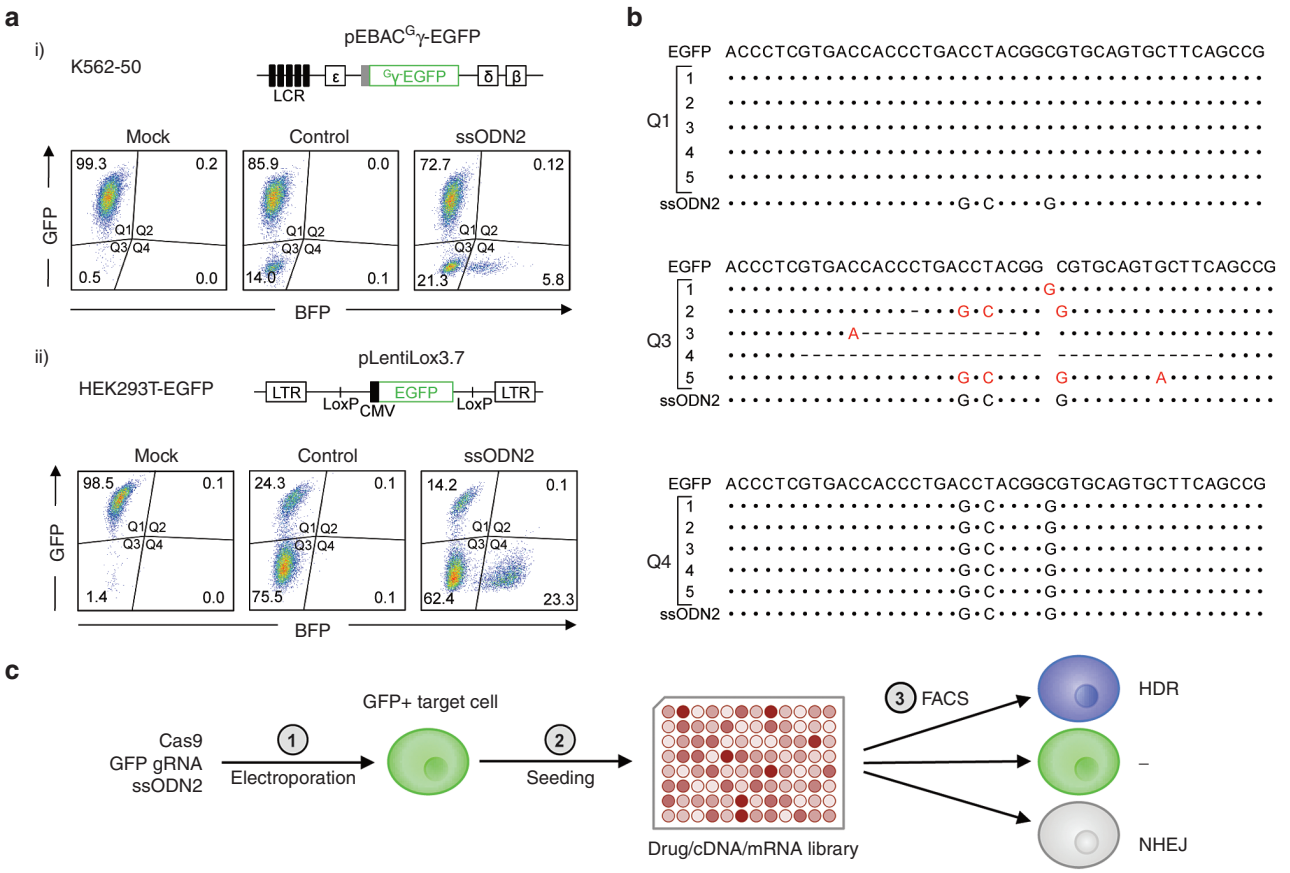

Figure 2 Verification of the GFP to BFP conversion assay. (a) Flow cytometric analysis of GFP to BFP conversion in K562-50 (i) and HEK293T-EGFP (ii) cells showing EGFP and BFP fluorescence 10 days after electroporation (mock = mock electroporation, control = Cas9/gRNA vector alone, ssODN2 = coelectroporation of Cas9/gRNA vector and ssODN2.). EGFP-modifications in target cells are shown above the flow cytometry data. K562-50 was derived from K562 cells carrying a modified human β-globin locus with EGFP replacing the γ-globin gene. HEK293-EGFP cells origin from HEK293T cells transduced with a lentiviral vector encoding GFP, followed by clonal expansion. (**b**) Verification of GFP to BFP conversion as a tool for quantification of HDR and NHEJ trough Sanger sequencing. Single-cell sorting of K562-50 cells from Q1, Q3, and Q4 populations as shown in **Figure 2a** (i) was performed for clonal analysis. Representative Sanger sequencing results from PCR amplicons of the EGFP chromophore region from five individual clones for each quadrant are shown. (Dashed lines represent deletions, insertions, and substitutions are highlighted in red). (**c**) Proposed scheme for a high-throughput screen for modulators of HDR activity. GFP to BFP conversion could be used to screen drug, mRNA or cDNA libraries for enhancers of HDR.

Astrid Glaser[1,2], Bradley McColl[1] and Jim Vadolas[1,2]

[1]Murdoch Childrens Research Institute, Royal Children's Hospital, Parkville, Victoria, Melbourne, Australia; [2]Department of Pediatrics, University of Melbourne, Royal Children's Hospital, Parkville, Victoria, Melbourne, Australia. Correspondence: Jim Vadolas, Murdoch Childrens Research Institute, EL5.4.30, 50 Flemington Road, Parkville, Victoria 3052, Australia. E-mail: jim.vadolas@mcri.edu.au

Acknowledgments The authors acknowledge the financial support from the National Health and Medical Research Council, the Murdoch Childrens Research Institute, the Victorian Government's Operational Infrastructure Support Program and Thalassaemia Australia. Kwaku Dad Abu-Bonsrah (Murdoch Childrens Research Institute, Parkville, Australia) kindly provided the px330-IRES-mCherry plasmid encoding Cas9 and the gRNA scaffold. The authors declare that they have no disclosures.

1. Doudna, JA and Charpentier, E (2014). Genome editing. The new frontier of genome engineering with CRISPR-Cas9. *Science* **346**: 1258096.
2. Ran, FA, Hsu, PD, Wright, J, Agarwala, V, Scott, DA and Zhang, F (2013). Genome engineering using the CRISPR-Cas9 system. *Nat Protoc* **8**: 2281–2308.
3. Kim, H and Kim, JS (2014). A guide to genome engineering with programmable nucleases. *Nat Rev Genet* **15**: 321–334.
4. De Ravin, SS, Reik, A, Liu, PQ, Li, L, Wu, X, Su, L *et al.* (2016). Targeted gene addition in human CD34(+) hematopoietic cells for correction of X-linked chronic granulomatous disease. *Nat Biotechnol* **34**: 424–429.
5. Yu, C, Liu, Y, Ma, T, Liu, K, Xu, S, Zhang, Y *et al.* (2015). Small molecules enhance CRISPR genome editing in pluripotent stem cells. *Cell Stem Cell* **16**: 142–147.
6. Chu, VT, Weber, T, Wefers, B, Wurst, W, Sander, S, Rajewsky, K *et al.* (2015). Increasing the efficiency of homology-directed repair for CRISPR-Cas9-induced precise gene editing in mammalian cells. *Nat Biotechnol* **33**: 543–548.
7. Maruyama, T, Dougan, SK, Truttmann, MC, Bilate, AM, Ingram, JR and Ploegh, HL (2015). Increasing the efficiency of precise genome editing with CRISPR-Cas9 by inhibition of nonhomologous end joining. *Nat Biotechnol* **33**: 538–542.
8. Certo, MT, Ryu, BY, Annis, JE, Garibov, M, Jarjour, J, Rawlings, DJ *et al.* (2011). Tracking genome engineering outcome at individual DNA breakpoints. *Nat Methods* **8**: 671–676.
9. Hendel, A, Kildebeck, EJ, Fine, EJ, Clark, JT, Punjya, N, Sebastiano, V *et al.* (2014). Quantifying genome-editing outcomes at endogenous loci with SMRT sequencing. *Cell Rep* **7**: 293–305.

10. Miyaoka, Y, Chan, AH, Judge, LM, Yoo, J, Huang, M, Nguyen, TD *et al.* (2014). Isolation of single-base genome-edited human iPS cells without antibiotic selection. *Nat Methods* **11**: 291–293.
11. Heim, R, Prasher, DC and Tsien, RY (1994). Wavelength mutations and posttranslational autoxidation of green fluorescent protein. *Proc Natl Acad Sci USA* **91**: 12501–12504.
12. Howden, SE, Voullaire, L, Wardan, H, Williamson, R and Vadolas, J (2008). Site-specific, Rep-mediated integration of the intact beta-globin locus in the human erythroleukaemic cell line K562. *Gene Ther* **15**: 1372–1383.
13. Arpino, JA, Reddington, SC, Halliwell, LM, Rizkallah, PJ and Jones, DD (2014). Random single amino acid deletion sampling unveils structural tolerance and the benefits of helical registry shift on GFP folding and structure. *Structure* **22**: 889–898.